Excessive tumor-elaborated VEGF and its neutralization define a lethal paraneoplastic syndrome

Alex K. Wong*, Myra Alfert*, Diego H. Castrillon*†, Qiong Shen*, Jocelyn Holash‡, George D. Yancopoulos‡, and Lynda Chin*§¶

*Department of Adult Oncology, Dana–Farber Cancer Institute, Boston, MA 02115; †Department of Pathology, Brigham and Women's Hospital, Boston, MA 02115; ‡Regeneron Pharmaceuticals, Inc., Tarrytown, NY 10591; and §Department of Dermatology, Harvard Medical School, Boston, MA 02115

Communicated by David M. Livingston, Dana–Farber Cancer Institute, Boston, MA, April 18, 2001 (received for review December 22, 2000)

Vascular endothelial growth factor (VEGF) is a potent endothelial cell mitogen and key regulator of both physiologic and pathologic (e.g., tumor) angiogenesis. In the course of studies designed to assess the ability of constitutive VEGF to block tumor regression in an inducible RAS melanoma model, mice implanted with VEGF-expressing tumors sustained high morbidity and mortality that were out of proportion to the tumor burden. Documented elevated serum levels of VEGF were associated with a lethal hepatic syndrome characterized by massive sinusoidal dilation and endothelial cell proliferation and apoptosis. Systemic levels of VEGF correlated with the severity of liver pathology and overall clinical compromise. A striking reversal of VEGF-induced liver pathology and prolonged survival were achieved by surgical excision of VEGF-secreting tumor or by systemic administration of a potent VEGF antagonist (VEGF-TRAP$_{R1R2}$), thus defining a paraneoplastic syndrome caused by excessive VEGF activity. Moreover, this VEGF-induced syndrome resembles peliosis hepatis, a rare human condition that is encountered in the setting of advanced malignancies, high-dose androgen therapy, and *Bartonella henselae* infection. Thus, our findings in the mouse have suggested an etiologic role for VEGF in this disease and may lead to diagnostic and therapeutic options for this debilitating condition in humans.

Paraneoplastic syndromes are disorders of host organ function at a site distal from the primary tumor and its metastases, and they reflect "pathologic" communication between tumor cells and the host. It is estimated that 7–10% of all patients with cancer will present with signs and symptoms of a paraneoplastic condition at the time of tumor diagnosis, although as many as 50% of these individuals may experience such a disorder at some point during their illness (1). The symptomatic manifestations of paraneoplastic syndromes may pose the most troublesome and threatening clinical problems that patients with cancer face. Diagnosis and treatment of paraneoplastic conditions can, therefore, contribute to an improved qualify of life, and in some cases, prolong life.

A constellation of symptoms is defined as a paraneoplastic syndrome when it is associated with the presence of actively growing tumor that elaborates a factor in excess into circulation, which, upon removal by tumor resection, results in the alleviation of systemic symptoms. By definition, such a factor should be overexpressed in tumor cells *in vivo* and/or produced by tumor cells *in vitro* (1). Many of these factors are proteins that are normally secreted to act locally in a paracrine fashion. However, when markedly overproduced by tumor cells, they enter the circulation and act on tissue distant from the production site (2).

Vascular endothelial growth factor (VEGF) is an endothelial cell-specific growth/survival factor. Not only does VEGF play an essential role in the normal development and differentiation of the vascular system (3), it also plays a key role in pathologic angiogenesis such as tumor angiogenesis. It has been demonstrated that many human tumor cell lines secrete VEGF protein *in vitro*, and the vast majority of primary human tumors show up-regulation of VEGF in the tumor cell compartment (3). On the other hand, expression of the VEGF receptors, VEGFR-1 and VEGFR-2, are typically found to be up-regulated in tumor-associated endothelial cells (3), which is consistent with the prime actions of VEGF as a paracrine factor. In the context of this study, it is notable that some patients with cancer possess readily detectable levels of VEGF in the serum and that such elevations are associated with poor clinical outcomes (3).

In the course of assessing the importance of VEGF in the maintenance of RAS-dependent tumor angiogenesis, we encountered a rapidly progressive and lethal phenotype that suggested an etiologic role for VEGF in the process. Specifically, we have demonstrated that the down-regulation of RAS expression in tumor cells leads to the regression of fully established melanomas accompanied by massive endothelial cell apoptosis (4). Because VEGF gene expression is regulated positively by RAS activation (5–7), we tested whether constitutive VEGF expression could modulate the collapse of tumor vasculature after down-regulation of RAS expression. Unexpectedly, mice implanted with these VEGF-overexpressing melanomas succumbed to a rapid demise accompanied by a constellation of symptoms associated with excessive circulating VEGF levels. The studies described here uncover a pathogenetic role for VEGF overexpression in this newly defined paraneoplastic syndrome and provide a potential avenue for therapeutic intervention.

Materials and Methods

Enforced VEGF-Expressing Melanoma (R545) and Glioma (C6) Cell Lines. R545 is a doxycycline-responsive melanoma cell line derived from a cutaneous melanoma arisen in a Tyr/Tet-RAS INK4a −/− mouse (4). R545 was maintained in medium supplemented with doxycycline (2 μg/ml) as described (4). The C6 glioma cell line used in these studies was available from Regeneron Pharmaceuticals (Tarrytown, NY). Both melanoma and glioma cell lines were transduced with LZRSpBMN-VEGF-IRES-GFP or LZRSpBMN-IRES-GFP (IRES, internal ribosome entry site; GFP, green flourescent protein) and purified populations were established by fluorescence-activated cell sorting (8).

Explant Tumor Mice with High Circulating Tumor-Derived VEGF Levels. Severe combined immunodeficient (SCID) mice, aged 6–8 weeks (Taconic Farms), were transplanted s.c. with 1×10^6 VEGF-expressing or GFP-expressing cells per site at two to four sites on the flanks. SCID mice injected with R545 melanoma

Abbreviations: VEGF, vascular endothelial growth factor; PCNA, proliferating cell nuclear antigen; TUNEL, terminal deoxynucleotidyltransferase-mediated dUTP nick end labeling; IHC, immunohistochemistry; GFP, green fluorescent protein.

¶To whom reprint requests should be addressed. E-mail: lynda_chin@dfci.harvard.edu.

The publication costs of this article were defrayed in part by page charge payment. This article must therefore be hereby marked "*advertisement*" in accordance with 18 U.S.C. §1734 solely to indicate this fact.

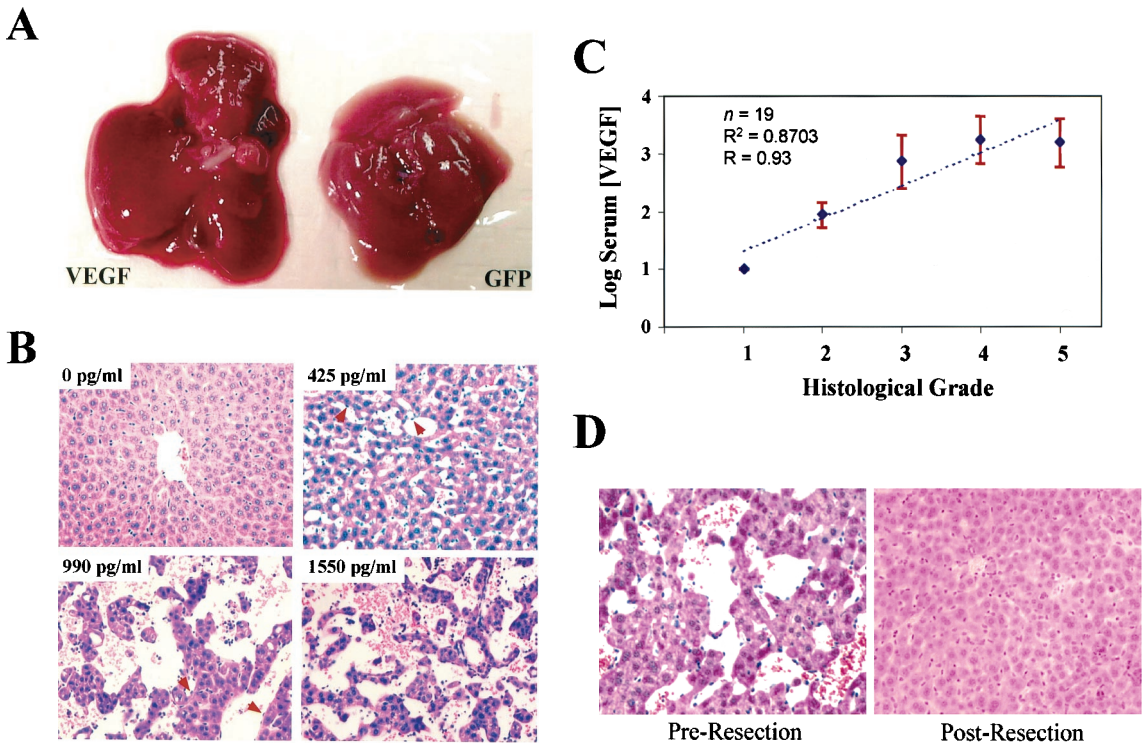

Fig. 1. Peliosis-like liver-specific pathology in mice bearing VEGF-expressing tumors. (*A*) Gross morphology of livers harvested from VEGF-melanoma mice (*Left*) and GFP-melanoma mice (*Right*). Note increased size and engorged appearance of liver from VEGF-melanoma mouse. (*B*) Representative photomicrographs of hematoxylin/eosin (H&E) sections of livers from GFP-melanoma mice (*Upper Left*) and livers from VEGF-melanoma mice (remaining three images). Note the dilatation of hepatic sinusoids with increasing severity correlating to detectable circulating VEGF levels (upper left corner of each image). Arrows, plump or sloughed endothelial cells. (*C*) Correlation between the severity of the liver pathology and the serum VEGF level in VEGF-melanoma mice. The histological grades are determined as follows: grade 1, indistinguishable from wild-type livers; grade 2, very slight sinusoidal dilatation, less than one cord (of hepatocytes) in thickness, but distinguishable from wild type by plump endothelial cells; grade 3, sinusoidal dilatation, mild, one to two cords in thickness; grade 4, sinusoidal dilatation, moderate, two to five cords in thickness; grade 5, sinusoidal dilatation, severe, has blood lakes and more than five cords thickness. The significance of the correlation is indicated by the correlation coefficient, $r = 0.93$. (*D*) Representative photomicrograph of hematoxylin/eosin sections of liver biopsied from the same mouse at two different time points. (*Left*) Liver was biopsied at the time when VEGF-expressing melanomas were resected from the mouse, which was 16 days after s.c. injection of tumor cells. (*Right*) Liver biopsied 21 days after the first biopsy, i.e., after removal of VEGF-expressing melanomas. Note the abnormal liver histology with characteristic sinusoidal dilatation (*Left*) has reversed to a relatively normal liver architecture (*Right*). (*B* and *D*, ×20.)

cells were maintained on doxycycline drinking water as described (4). To measure systemic VEGF levels, whole blood samples were obtained by retro-orbital bleed and allowed to clot for either 1 h at room temperature or overnight at 4°C. Serum was analyzed in duplicate with the mouse VEGF Quantikine M Immunoassay Kit (Kit no. MMV00, R & D Systems) according to the manufacturer's protocol (which quantitates both natural and recombinant mouse VEGF).

Histological Analysis and Immunohistochemistry (IHC). For paraffin sections, tissue and tumor samples were immersion-fixed in 10% (vol/vol) buffered formalin and embedded in paraffin. For cryostat sections, tissue and tumor samples were fixed in 4% (vol/vol) paraformaldehyde, equilibrated in 17% (wt/vol) sucrose, and frozen in Tissue-Tek OCT compound (EM Science). For ultrastructural analysis, liver samples were cut into 1-mm blocks and immediately submersed in Karnovsky's fixative (EM Science). Routine hematoxylin/eosin treatment and electron microscopy were performed by D.H.C. and the pathology laboratory at the Brigham and Women's Hospital (Boston, MA). Anti-proliferating cell nuclear antigen (PCNA; 1:50; Santa Cruz Biotechnology), anti-BrdUrd (Oncogene Science), and anti-CD31 (1:50; PharMingen) IHC and terminal deoxynucleotidyl-transferase-mediated dUTP nick end labeling (TUNEL; Intergen, Purchase, NY) were performed according to the manufacturers' protocols.

RNA *in Situ* Hybridization. Dig-labeled antisense riboprobes were hybridized to cryostat sections of tissues as described (9). For hFlk-1, pBS-hFLK1(full)_1.mv (Regeneron Pharmaceuticals), which contains full-length hFlk-1 cDNA, was used to generate the antisense probe.

VEGF-Inhibitor Treatment. VEGF-TRAP$_{R1R2}$ (Regeneron Pharmaceuticals) or placebo [5% (vol/vol) PBS/glycerol] was administered s.c. at a dose of 25 mg/kg every 2 days commencing on the day when tumors became palpable. The dosing was administered every day after 50% of the placebo-treated mice had died and maintained on an every-day schedule until the end of the study.

Statistical Analysis. *P* values were calculated by using a two-tailed *t* test. Kaplan–Meier survival curves were constructed with the PRISM software (GraphPad, San Diego).

Results and Discussion

Down-regulation of activated RAS expression leads to regression of fully established melanomas caused in part by a loss of proangiogenic support (4). In the course of assessing whether enforced VEGF expression can block RAS-mediated collapse in tumor vasculature, it was noted that mice harboring VEGF-expressing melanomas (designated "VEGF-melanoma mice") experienced high mortality and were generally moribund only 14

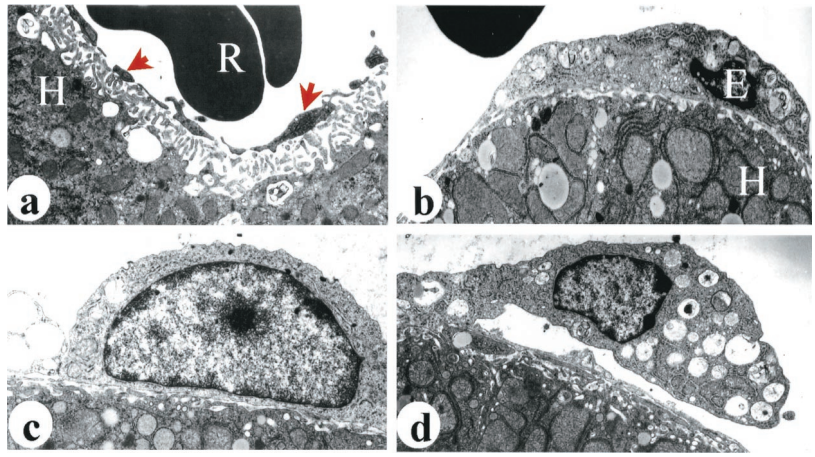

Fig. 2. Ultrastructural analysis of VEGF-mediated liver pathology. (*a*) Normal liver. Note the thinly fenestrated endothelial cell extensions (red arrows) in close contact with hepatocyte (H) by means of finger-like projections (microvilli) in the space of Disse. R, red blood cells in the sinusoidal space. (*b–d*) Abnormal liver from VEGF-melanoma mouse. (*b*) Plump endothelial cell lining sinusoid. E, endothelial cell. (*c*) Rounding up of endothelial cell with retraction of cytoplasmic extensions. (*d*) Endothelial cell in the process of sloughing off. Detaching cell, although clearly abnormal with numerous cytoplasmic inclusions, was determined to be of endothelial origin by the presence of tight junctions at the points of contact with endothelial cell neighbors (not shown).

days after tumor-cell injection. In contrast, control mice with GFP-expressing melanomas (designated ''GFP-melanoma mice'') remained healthy for several weeks up to the point of maximal tumor growth, which necessitated killing. We have shown elsewhere that VEGF-expressing melanoma cell lines form tumors at a faster rate and achieve a larger size relative to GFP controls (4); however, the clinical compromise of the VEGF-melanoma mice seemed to be out of proportion to their increased tumor burden, suggesting that high tumor-derived VEGF levels could be responsible for the rapid demise. Along these lines, it has been shown recently that i.v. administration of adenovirus-encoding VEGF (Ad-VEGF) can achieve massively high circulating VEGF levels in mice, ranging from 10^3 to 10^6 pg/ml within 24 h. These Ad-VEGF-infected mice succumb rapidly in a dose-dependent manner within 2–7 days to a fatal syndrome of generalized organ edema, which is consistent with the role of VEGF in vascular permeability (10).

A sensitive ELISA assay was used to determine whether VEGF-melanomas elaborated detectable circulating levels of VEGF. The serum VEGF levels in nonmelanoma-bearing mice and GFP-melanoma mice ranged from undetectable to <150 pg/ml ($n = 7$ mice; mean VEGF level = 59 pg/ml), whereas levels in VEGF-melanoma mice ranged from 365 pg/ml to 8,572 pg/ml ($n = 19$ mice; mean VEGF level = 2,316 pg/ml). Time course measurements revealed a gradual increase in serum VEGF levels over 10–14 days, which is commensurate with a growing tumor burden, reaching peak levels at the time of demise (data not shown). Postmortem gross and microscopic examinations were unremarkable for all major organs except for the livers from VEGF-melanoma mice that, in all cases, were found to be significantly engorged with blood (Fig. 1*A*). Histological analysis revealed that the affected livers had severely disrupted parenchymal architecture highlighted by massively dilated sinusoidal spaces lined by prominent endothelial cells with sloughing (Fig. 1*B*). Diffuse sinusoidal dilatation is the characteristic feature of peliosis hepatis, a human condition of unknown etiology that has been described in association with *Bartonella henselae* infection, long-term high-dose androgen therapy, or rarely with advanced cancers (11). That excessive VEGF could be playing an etiologic role was suggested by the correlation between rising serum VEGF levels and the severity of the liver pathology ($r = 0.93$, Fig. 1*C*) and overall clinical compromise (gauged by an earlier onset of ill appearance, inactivity, and weight loss; data not shown). These findings provide evidence that high-serum VEGF may be playing a key etiologic role in this life-threatening syndrome. Along these lines, it is notable that *B. henselae* is the causative agent for bacillary angiomatosis, a condition characterized by development of pseudoneoplastic angioproliferative lesions (12), presumably caused by the elaboration of angiogenic factors, and peliosis hepatis in immunosuppressed patients (13, 14). Additionally, a similar etiologic link to androgen-induced toxicity is strengthened by the observation that sex-steroid hormones can regulate VEGF gene expression (15–17).

Next, we determined whether the phenotypic impact of elevated systemic VEGF levels was specific to melanoma *per se* by monitoring the response to explant tumors derived from C6 rat glioma cells similarly engineered to express constitutively VEGF or GFP. Under experimental conditions identical to those described above, VEGF-glioma mice were moribund within 11–12 days, while GFP-glioma mice appeared healthy up to the time of killing on day 19 ($n = 4$ each). Microscopic analysis of the livers revealed a severe sinusoidal dilatation only in the VEGF-glioma mice (data not shown), indicating that the phenotype was not tumor type-specific.

To fortify the link between circulating VEGF level and the observed liver pathology, serial liver biopsies and serum VEGF levels were monitored in VEGF-melanoma mice before and after tumor resection. At the time when VEGF-melanoma mice were documented to have elevated serum VEGF levels (i.e., >59 pg/ml, the mean level detected in GFP-melanoma mice), liver biopsies were performed, and tumors were resected under anesthesia. Of 11 mice, 5 succumbed to immediate perioperative complications without recovering from anesthesia. Of these five mice, four had serum VEGF levels above 1,000 pg/ml (mean = 855 pg/ml, $n = 5$), which established a correlation between high VEGF levels and overall surgical compromise. In comparison, mice with more moderate VEGF levels (mean = 417 pg/ml, $n = 6$) survived surgery and recovered well, with only one of six mice dying 2 weeks after surgery for unknown reasons. When killed 3 weeks later, the remaining five mice were clinically healthy and showed a reduction in serum VEGF levels to low or undetectable levels (mean = 2.3 pg/ml, $n = 5$). Serial histological analyses of liver biopsies harvested from the same animals showed severe sinusoidal dilation and plump endothelial cells with sloughing into the sinusoidal space at the time of tumor resection and normal liver histology 3 weeks after tumor resection (Fig. 1*d*). Thus, the liver condition correlates tightly with VEGF levels and is completely reversible.

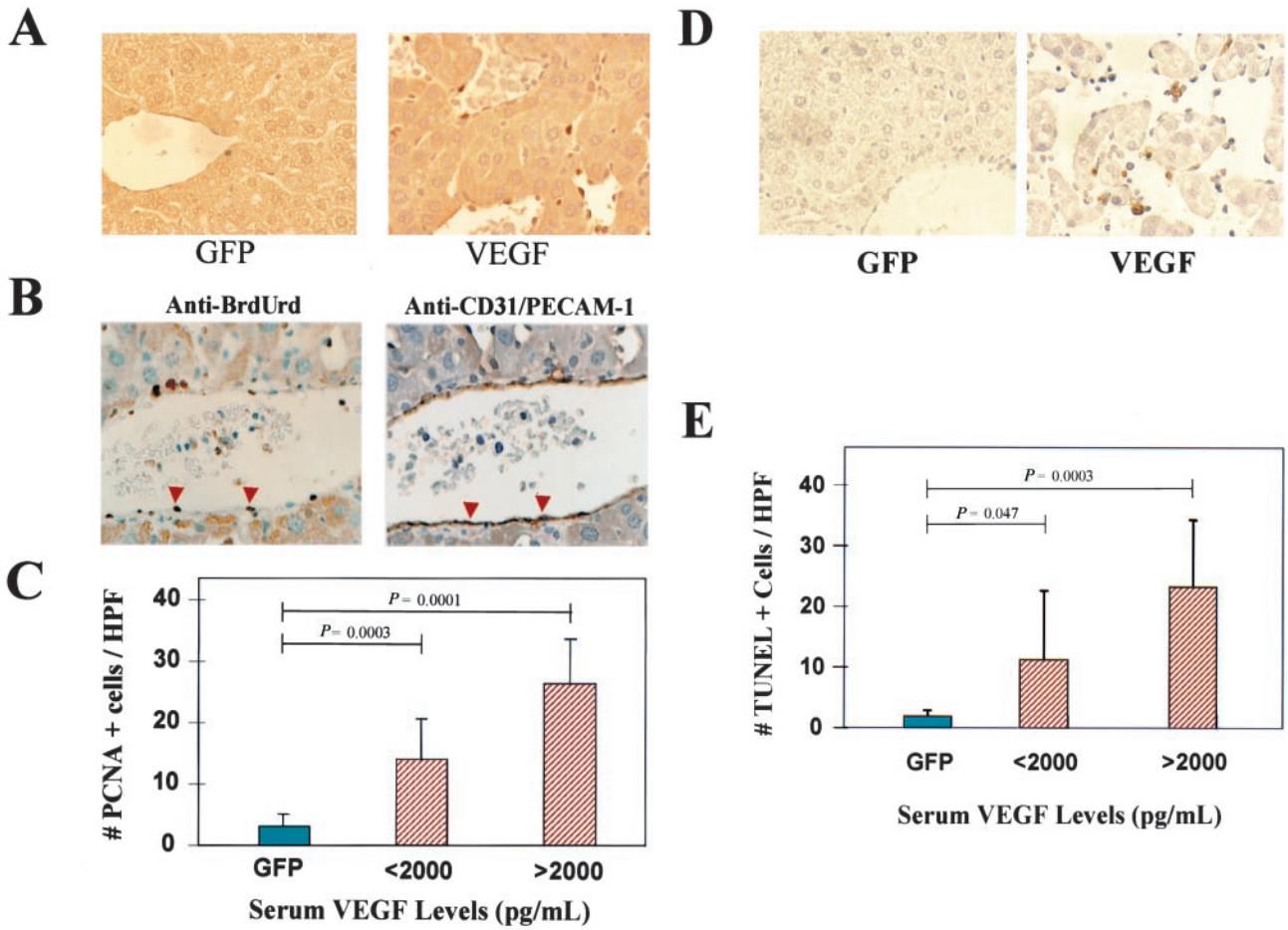

Fig. 3. Hepatic endothelial cells are undergoing proliferation and apoptosis in VEGF-tumor mice. (*A*) Representative photomicrograph of anti-PCNA IHC performed on liver sections from GFP-melanoma (*Left*) and VEGF-melanoma (*Right*) mice. Note the presence of the PCNA-positive cells lining the sinusoidal space in the liver of VEGF-tumor mice only. (*B*) Photomicrographs of consecutive sections of liver from VEGF-melanoma mice, stained for BrdUrd and endothelial cell-specific antibody CD31. Note presence of BrdUrd-positive cells that exhibit cytoplasmic immunoreactivity to CD31 (red arrows), indicating that these proliferating cells are endothelial in origin. (*C*) Histogrammatic representation of the number of PCNA-positive cells in the livers of GFP-melanoma mice (green bar) or in the livers of VEGF-melanoma mice (red striped bars) with various circulating VEGF levels ($P = 0.0003$ and $P = 0.0001$, respectively). HPF, high power field. (*D*) Representative photomicrographs of TUNEL IHC on liver sections from GFP-melanoma (*Left*) and VEGF-melanoma (*Right*) mice. Note the presence of TUNEL-positive cells only in the livers of VEGF-melanoma mice. (*E*) Histogrammatic representation of the number of TUNEL-positive cells in the livers of GFP-melanoma mice (green bar) or in the livers of VEGF-melanoma mice (red striped bars) with various circulating VEGF levels ($P = 0.047$ and $P = 0.0003$, respectively). (*A*, *B*, and *D*, ×40.)

To characterize the histogenesis of this peliosis-like syndrome better, ultrastructural analysis of the livers was performed. As shown in Fig. 2*a*, the normal sinusoidal space is lined by thin cytoplastic extensions of endothelial cells (arrows), separated by fenestrae. In contrast, the sinusoidal space in livers from VEGF-tumor mice were lined by plump, rounded endothelial cells with retracted cytoplastic extensions (Fig. 2 *b* and *c*). Some of the endothelial cells appeared to be in the process of detaching from the endothelium (Fig. 2*d*), and many detached cells (with characteristic features of endothelial cells) were observed in the sinusoidal spaces (data not shown). These ultrastructural findings, coupled with the light microscopic (Fig. 1) and IHC (Fig. 3) studies, support the hypothesis that high circulating VEGF levels lead to the detachment of hepatic sinusoidal endothelial cells into the dilated sinusoidal space.

To explore the pathophysiological actions of VEGF on sinusoidal endothelial cells, we examined their proliferative and apoptotic rates. Consistent with the role of VEGF as a potent endothelial cell mitogen, histological analysis of liver sections from VEGF-tumor mice revealed the presence of mitotic figures localizing to the lining of dilated sinusoids (data not shown). Correspondingly, anti-PCNA IHC of GFP-melanoma and VEGF-melanoma liver sections ($n = 7$ and $n = 19$, respectively) showed active proliferation along the lining of the hepatic sinusoids in VEGF-melanoma livers only. That these proliferating cells were, indeed, endothelial cells was confirmed by anti-BrdUrd and anti-CD31 IHC on consecutive sections (Fig. 3*B*). The rate of endothelial cell proliferation correlated positively with serum VEGF levels ($P = 0.0001$, Fig. 3*C*). VEGF also serves as a potent endothelial cell-survival factor (18–21). However, the presence of pyknotic nuclei and TUNEL-positive cells in the sinusoids revealed a high rate of apoptosis in VEGF-tumor livers only (Fig. 3*D*). This picture was consistent with the activation of apoptosis upon sloughing of endothelial cells, suggesting that reentry into the cell cycle and disruption of cell contacts may elicit an apoptotic response despite high VEGF levels (18–21). The rate of apoptosis correlated positively with serum VEGF levels ($P = 0.0003$, Fig. 3*E*). Together, these findings suggest that high circulating VEGF levels can drive hepatic endothelial cell proliferation and apoptosis *in vivo*.

VEGF exerts its functions through two known receptor tyrosine kinases, VEGFR-1 (Flt-1) or VEGFR-2 (KDR/Flk-1), both expressed predominantly on vascular endothelium of large and small vessels (22). Although VEGF can bind to both Flt-1

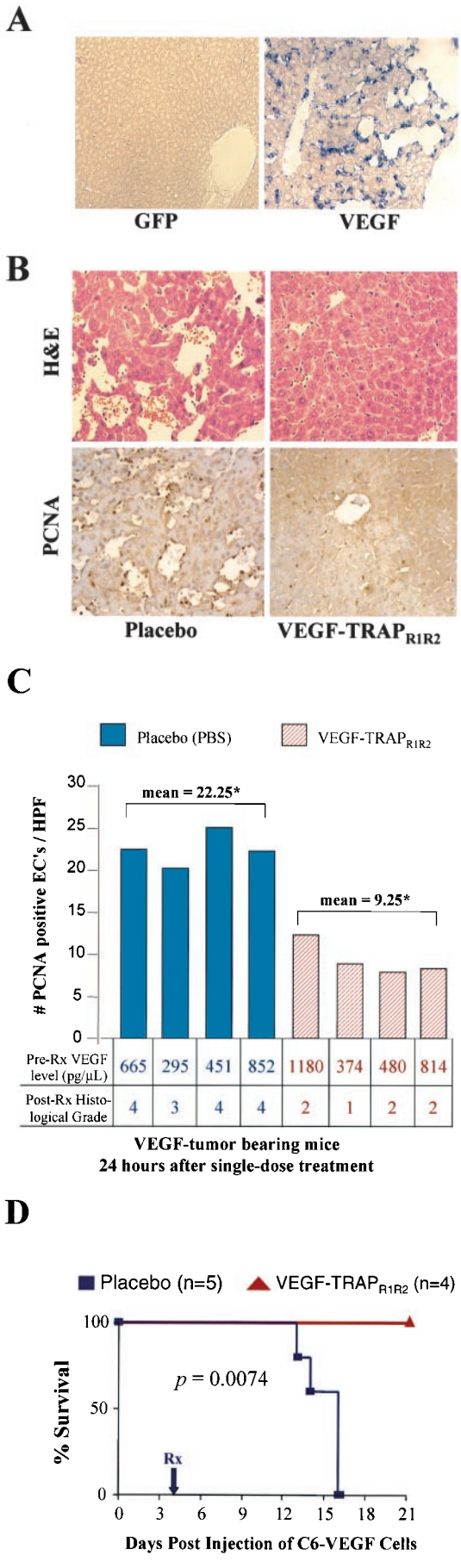

and KDR/Flk-1 with high affinity, only KDR/Flk-1 undergoes strong ligand-dependent tyrosine phosphorylation in intact cells, whereas Flt-1 reveals a weak or undetectable response (23). Interaction with KDR/Flk-1 is thought to be required for induction of the full spectrum of VEGF biological responses (24). In addition, other studies have shown that VEGF can up-regulate KDR/Flk-1 expression *in vitro* (25). Thus, we sought to determine whether KDR/Flk-1 is indeed expressed and up-regulated in VEGF-melanoma mice with high circulating levels of VEGF. As shown in Fig. 4*A*, RNA *in situ* hybridization with antisense hFLK1 confirmed a dramatic induction of KDR/Flk-1 expression localizing strictly to the sinusoidal lining of livers harvested from VEGF-tumor mice. A survey of other organs (muscle, kidney, lung, testis, and intestine) did not reveal a significant induction of KDR/Flk-1 expression (data not shown). The specific liver pathology observed in the VEGF-tumor mice over the duration of our studies correlates with the induction of Flk-1/KDR expression on hepatic endothelial cells. It should be noted that we have not ruled out the possibility that prolonged elevation of VEGF could elicit similar changes in endothelial cells of other organ systems.

The results above suggested that induction of KDR/Flk-1 in hepatic endothelial cells render them specifically sensitive to the biological action of VEGF. We then asked whether a blockade of VEGF-dependent activation of KDR/Flk-1 by systemic VEGF-TRAP$_{R1R2}$ administration, a recombinantly engineered version of a soluble VEGF-receptor fusion that potently binds and blocks VEGF actions *in vivo* (S. Davis and G. D. Yancopoulos, unpublished data), could modulate or alleviate some of the consequences of the elevated VEGF level in our model. To this end, VEGF-melanoma mice were followed until they developed systemic VEGF levels that were high enough to ensure moderate to severe liver pathology (i.e., >500 pg/ml). These mice were then given a s.c. bolus (25 mg/kg) of either VEGF-TRAP$_{R1R2}$ ($n = 4$) or an equivalent volume of placebo ($n = 4$). Mice were killed 24 h later, and livers were harvested for histological analysis. Surprisingly, a single-dose treatment with VEGF-TRAP$_{R1R2}$ significantly attenuated the liver pathology as measured by a histological grade of peliosis-like changes ($P < 0.001$) and the extent of endothelial cell proliferation ($P < 0.0001$; Fig. 4 *B* and *C*). This result and the findings described above strongly suggest that the liver pathology is a direct paraneoplastic consequence of VEGF activity. Moreover, because acute administration of VEGF-TRAP$_{R1R2}$ did not alter

Fig. 4. Specific and systemic blockage of VEGF reverses peliosis-like liver pathology and prolongs the survival of VEGF-tumor mice. (*A*) KDR/Flk-1 receptor expression by RNA *in situ* hybridization performed on liver sections from GFP-melanoma (*Left*) and VEGF-melanoma (*Right*) mice. Note the signals localizing to regions lining the sinusoidal space. (*B*) Representative photomicrograph of hematoxylin/eosin (H&E) and PCNA-stained sections of livers from VEGF-melanoma mice treated with placebo (*Left*) or VEGF-TRAP$_{R1R2}$ (*Right*). Note the relatively normal architecture in VEGF-TRAP$_{R1R2}$-treated livers. (*C*) Histogrammatic representation of the number of PCNA-positive endothelial cells per high-power field in livers of VEGF-melanoma mice treated with a single dose of placebo (blue bars) or VEGF-TRAP$_{R1R2}$ (red striped bars). Below the horizontal axis, pretreatment serum VEGF levels and post-treatment histological grades are indicated. Note that despite comparable or higher pretreatment VEGF levels, VEGF-TRAP$_{R1R2}$-treated animals exhibited a much milder degree of liver pathology as measured by histological grade ($P = 0.001$) and PCNA counts ($P = 0.0001$) HPF, high power field. (*D*) Kaplan–Meier survival curves of animals bearing tumors from C6-VEGF cells on continuous placebo or VEGF-TRAP$_{R1R2}$ treatment. Note the significant prolongation of life when treated with inhibitor. At the time of killing (day 21), all four treated mice were outwardly healthy despite the large tumor burden. Similar treatment trials were performed with identical outcomes with R545-VEGF cells. Total number of treatment trials was three. (*A Right*, ×40; *A Left*, *B Left*, and *B Right*, ×20.)

acutely the tumor burden, therapeutic reversal of the peliosis-like phenotype indicates that this paraneoplastic state is linked tightly to VEGF toxicity rather than tumor burden.

Given the significant impact of single-dose VEGF-TRAP$_{R1R2}$ on liver pathology, we determined whether repeated and continuous neutralization of VEGF activity *in vivo* impacts on VEGF-induced morbidity and mortality. As shown in Fig. 4*D*, administration of VEGF-TRAP$_{R1R2}$ improved survival dramatically. VEGF-glioma mice receiving placebo succumbed by day 16 ($n = 5$), whereas those administered VEGF-TRAP$_{R1R2}$ ($n = 4$) remained in good health until the termination of the therapeutic trial. Similar survival curves were generated in studies employing a VEGF-melanoma cell line (data not shown). Because the beneficial effects of VEGF-TRAP$_{R1R2}$ treatment were clinically and statistically profound, and because the size of VEGF-tumors approached protocol limits by 21 days, we did not prolong our studies beyond this point. Clinically, VEGF-TRAP$_{R1R2}$-treated animals were healthy at day 21. However, when VEGF-TRAP$_{R1R2}$ therapy was discontinued, the animals became ill and died within 2–5 days (data not shown), bolstering the notion that VEGF toxicity was the primary mediator of death.

The constellation of symptoms observed in VEGF-tumor mice constitutes a newly defined paraneoplastic syndrome and raises the possibility of an equivalent condition in patients with cancer possessing advanced VEGF-secreting tumors. It is worth noting that peliosis hepatis has been observed in patients with cancer. For example, several case reports have described patients with unexplained peliosis hepatis who later were found to have underlying malignancies at autopsy. In one instance, malignant histocytosis of the liver and bone marrow was discovered (26). In another study, a neoplasm was detected in five of nine cases (27). Others have also described the development of peliosis in the setting of known malignancies, including renal cell carcinoma, pancreatic cancer, and Wilm's tumor (28–30). With respect to VEGF as a mediator of this particular paraneoplastic syndrome, it has been well established that many human cancers secrete VEGF, and that in some instances, elevated levels of VEGF can be detected in sera of patients with advanced malignancy (31–34). Moreover, there seems to be a correlation between serum VEGF levels and prognosis (33, 35–37). For example, in one study, patients with metastatic nasopharyngeal carcinoma possessed a median serum VEGF level of 958.6 pg/ml, compared with 371.0 pg/ml and 375.6 pg/ml in healthy controls and patients with cancer with nonmetastatic disease, respectively (36). In a separate study of 614 patients with colorectal cancer and 91 healthy volunteers, it was shown that patients with serum VEGF levels of >465 pg/ml (the upper limit of the 95th percentile of healthy individuals) had significantly reduced overall survival relative to patients with serum VEGF levels of <465 pg/ml. Furthermore, within the subgroup of patients who had carcinoma localized to the colon and serum VEGF levels >465 pg/ml, high serum VEGF correlated directly with reduced overall survival (32). Although the poorer outcome in these patients is likely due to a multitude of factors, the findings of this report raise the possibility that tumor-associated morbidity and mortality in such patients can be attributed in part to high circulating levels of VEGF. Such observations should prompt the measurement of serum VEGF levels and liver function in patients with excessive tumor burden and encourage the use of anti-VEGF therapy in those cases. In settings other than cancer, the observations of similar pathological presentation in *B. henselae* infection and long-term high-dose androgen therapy imply a pathophysiological role for VEGF in these conditions and, therefore, suggest equivalently profound therapeutic opportunities for the systemic blockage of VEGF activity.

We thank Dr. R. A. DePinho for a critical reading of the manuscript. This work is supported by National Institutes of Health Grant K08AR02104-01 and National Cancer Institute Grant U01CA84313-01. A.K.W. is a Howard Hughes Medical Institute Medical Student Research Fellow. D.H.C. is supported by National Institutes of Health Grant KO8CA84044. L.C. is a V Foundation scholar. Support from the Dana–Farber Cancer Institute to L.C. is acknowledged.

1. Nathanson, L. & Hall, T. C. (1997) *Semin. Oncol.* **24,** 265–268.
2. Odell, W. D. (1997) *Semin. Oncol.* **24,** 299–317.
3. Ferrara, N. (1999) *Curr. Top. Microbiol. Immunol.* **237,** 1–30.
4. Chin, L., Tam, A., Pomerantz, J., Wong, M., Holash, J., Bardeesy, N., Shen, Q., O'Hagan, R., Pantginis, J., Zhou, H., *et al*. (1999) *Nature (London)* **400,** 468–472.
5. Rak, J., Mitsuhashi, Y., Bayko, L., Filmus, J., Shirasawa, S., Sasazuki, T. & Kerbel, R. S. (1995) *Cancer Res.* **55,** 4575–4580.
6. Arbiser, J. L., Moses, M. A., Fernandez, C. A., Ghiso, N., Cao, Y., Klauber, N., Frank, D., Brownlee, M., Flynn, E., Parangi, S., *et al*. (1997) *Proc. Natl. Acad. Sci. USA* **94,** 861–866.
7. Okada, F., Rak, J. W., Croix, B. S., Lieubeau, B., Kaya, M., Roncari, L., Shirasawa, S., Sasazuki, T. & Kerbel, R. S. (1998) *Proc. Natl. Acad. Sci. USA* **95,** 3609–3614.
8. Cheng, L., Fu, J., Tsukamoto, A. & Hawley, R. G. (1996) *Nat. Biotechnol.* **14,** 606–609.
9. Ma, Q., Chen, Z., del Barco Barrantes, I., de la Pompa, J. L. & Anderson, D. J. (1998) *Neuron* **20,** 469–482.
10. Thurston, G., Rudge, J. S., Ioffe, E., Zhou, H., Ross, L., Croll, S. D., Glazer, N., Holash, J., McDonald, D. M. & Yancopoulos, G. D. (2000) *Nat. Med.* **6,** 460–463.
11. Schafer, D. & Sorrell, M. (1998) in *Sleisenger and Fordtran's Gastrointestinal and Liver Disease*, eds. Feldman, M. & Sleisenger, M. (Saunders, Philadelphia), pp. 1195–1196.
12. Relman, D. A., Loutit, J. S., Schmidt, T. M., Falkow, S. & Tompkins, L. S. (1990) *N. Engl. J. Med.* **323,** 1573–1580.
13. Perkocha, L. A., Geaghan, S. M., Yen, T. S., Nishimura, S. L., Chan, S. P., Garcia-Kennedy, R., Honda, G., Stoloff, A. C., Klein, H. Z., Goldman, R. L., *et al*. (1990) *N. Engl. J. Med.* **323,** 1581–1586.
14. Tappero, J. W., Mohle-Boetani, J., Koehler, J. E., Swaminathan, B., Berger, T. G., LeBoit, P. E., Smith, L. L., Wenger, J. D., Pinner, R. W., Kemper, C. A., *et al*. (1993) *J. Am. Med. Assoc.* **269,** 770–775.
15. Greb, R. R., Heikinheimo, O., Williams, R. F., Hodgen, G. D. & Goodman, A. L. (1997) *Hum. Reprod.* **12,** 1280–1292.
16. Hazzard, T. M., Molskness, T. A., Chaffin, C. L. & Stouffer, R. L. (1999) *Mol. Hum. Reprod.* **5,** 1115–1121.
17. Hyder, S. M., Murthy, L. & Stancel, G. M. (1998) *Cancer Res.* **58,** 392–395.
18. Yuan, F., Chen, Y., Dellian, M., Safabakhsh, N., Ferrara, N. & Jain, R. K. (1996) *Proc. Natl. Acad. Sci. USA* **93,** 14765–14770.
19. Benjamin, L. E. & Keshet, E. (1997) *Proc. Natl. Acad. Sci. USA* **94,** 8761–8766.
20. Gerber, H. P., McMurtrey, A., Kowalski, J., Yan, M., Keyt, B. A., Dixit, V. & Ferrara, N. (1998) *J. Biol. Chem.* **273,** 30336–30343.
21. Fujio, Y. & Walsh, K. (1999) *J. Biol. Chem.* **274,** 16349–16354.
22. Neufeld, G., Cohen, T., Gengrinovitch, S. & Poltorak, Z. (1999) *FASEB J.* **13,** 9–22.
23. Waltenberger, J., Claesson-Welsh, L., Siegbahn, A., Shibuya, M. & Heldin, C. H. (1994) *J. Biol. Chem.* **269,** 26988–26995.
24. Ferrara, N. & Davis-Smyth, T. (1997) *Endocr. Rev.* **18,** 4–25.
25. Shen, B. Q., Lee, D. Y., Gerber, H. P., Keyt, B. A., Ferrara, N. & Zioncheck, T. F. (1998) *J. Biol. Chem.* **273,** 29979–29985.
26. Fine, K. D., Solano, M., Polter, D. E. & Tillery, G. W. (1995) *Am. J. Gastroenterol.* **90,** 485–488.
27. Karasawa, T., Shikata, T. & Smith, R. D. (1979) *Acta Pathol. Jpn.* **29,** 457–469.
28. Otani, M., Ohaki, Y., Nakatani, Y., Ito, E., Shimoyama, K. & Misugi, K. (1992) *Acta Pathol. Jpn.* **42,** 62–68.
29. Godoy, P. & Bambirra, E. A. (1979) *AMB Rev. Assoc. Med. Bras.* **25,** 205–207.
30. Bjork, O., Eklof, O., Willi, U. & Ahstrom, L. (1985) *Acta Radiol. Diagn. (Stockh.)* **26,** 589–597.
31. Salven, P., Manpaa, H., Orpana, A., Alitalo, K. & Joensuu, H. (1997) *Clin. Cancer Res.* **3,** 647–651.
32. Takigawa, N., Segawa, Y., Fujimoto, N., Hotta, K. & Eguchi, K. (1998) *Anticancer Res.* **18,** 1251–1254.
33. Kraft, A., Weindel, K., Ochs, A., Marth, C., Zmija, J., Schumacher, P., Unger, C., Marme, D. & Gastl, G. (1999) *Cancer* **85,** 178–187.
34. Riedel, F., Gotte, K., Schwalb, J., Wirtz, H., Bergler, W. & Hormann, K. (2000) *Eur. Arch. Otorhinolaryngol.* **257,** 332–336.
35. Salven, P., Teerenhovi, L. & Joensuu, H. (1997) *Blood* **90,** 3167–3172.
36. Qian, C. N., Zhang, C. Q., Guo, X., Hong, M. H., Cao, S. M., Mai, W. Y., Min, H. Q. & Zeng, Y. X. (2000) *Cancer* **88,** 255–261.
37. Werther, K., Christensen, I. J., Brunner, N., Nielsen, H. J. & Danish, R. C. C. (2000) *Eur. J. Surg. Oncol.* **26,** 657–662.